Published in final edited form as:
Mol Cell. 2008 July 25; 31(2): 255–265. doi:10.1016/j.molcel.2008.06.014.

Targeting Bcl-2-IP3 Receptor Interaction to Reverse Bcl-2's Inhibition of Apoptotic Calcium Signals

Yi-Ping Rong[1,2], **Ademuyiwa S. Aromolaran**[4], **Geert Bultynck**[5], **Fei Zhong**[1,2], **Xiang Li**[3], **Karen McColl**[1,2], **Shigemi Matsuyama**[1,2], **Stephan Herlitze**[3], **H. Llewelyn Roderick**[6,7], **Martin D. Bootman**[6], **Gregory A. Mignery**[4], **Jan B. Parys**[5], **Humbert De Smedt**[5], and **Clark W. Distelhorst**[1,2,*]

[1]Department of Medicine, Case Western Reserve University, Cleveland, OH 44106, USA

[2]Department of Pharmacology, Case Western Reserve University, Cleveland, OH 44106, USA

[3]Department of Neuroscience, Case Western Reserve University, Cleveland, OH 44106, USA

[4]Department of Physiology, Stritch School of Medicine, Loyola University Chicago, Maywood, IL 60153, USA

[5]Laboratory of Molecular Signalling, Division of Physiology, K.U. Leuven Campus Gasthuisberg O/N1, B3000 Leuven, Belgium

[6]Laboratory of Molecular and Cellular Signaling, Babraham Institute, Cambridge CB2 4AT, UK

[7]Department of Pharmacology, University of Cambridge, Cambridge CB2 1PD, UK

SUMMARY

The antiapoptotic protein Bcl-2 inhibits Ca^{2+} release from the endoplasmic reticulum (ER). One proposed mechanism involves an interaction of Bcl-2 with the inositol 1,4,5-trisphosphate receptor (IP3R) Ca^{2+} channel localized with Bcl-2 on the ER. Here we document Bcl-2-IP3R interaction within cells by FRET and identify a Bcl-2 interacting region in the regulatory and coupling domain of the IP3R. A peptide based on this IP3R sequence displaced Bcl-2 from the IP3R and reversed Bcl-2-mediated inhibition of IP3R channel activity in vitro, IP3-induced ER Ca^{2+} release in permeabilized cells, and cell-permeable IP3 ester-induced Ca^{2+} elevation in intact cells. This peptide also reversed Bcl-2's inhibition of T cell receptor-induced Ca^{2+} elevation and apoptosis. Thus, the interaction of Bcl-2 with IP3Rs contributes to the regulation of proapoptotic Ca^{2+} signals by Bcl-2, suggesting the Bcl-2-IP3R interaction as a potential therapeutic target in diseases associated with Bcl-2's inhibition of cell death.

INTRODUCTION

Bcl-2 family proteins regulate cell death and survival (Cory and Adams, 2002; Danial and Korsmeyer, 2004). The founding member, Bcl-2, preserves mitochondrial integrity and inhibits apoptosis induction by diverse stimuli in part by inhibiting Ca^{2+} release from the endoplasmic reticulum (ER) (Giacomello et al., 2007; Pinton and Rizzuto, 2006; Rong and Distelhorst, 2008). Ca^{2+} elevation activates Ca^{2+}-sensitive proteases and endonucleases and triggers permeability transition and cytochrome *c* release in nearby mitochondria

*Correspondence: clark.distelhorst@case.edu.

SUPPLEMENTAL DATA

The Supplemental Data include Supplemental Experimental Procedures and six figures and can be found with this article online at http://www.molecule.org/cgi/content/full/31/2/255/DC1/.

(Giacomello et al., 2007; Hanson et al., 2004; Orrenius et al., 2003; Pinton and Rizzuto, 2006). Ca^{2+} oscillations, on the other hand, activate prosurvival transcription factors and increase mitochondrial metabolism. Although Bcl-2 and Bcl-X_L inhibit sustained Ca^{2+} elevation, they enhance Ca^{2+} oscillations (Li et al., 2007; Palmer et al., 2004; White et al., 2005; Zhong et al., 2006), indicating the versatility of their regulatory actions on Ca^{2+} signaling to promote cell survival. The inhibition of sustained ER Ca^{2+} release by Bcl-2 has been attributed to a Bcl-2-imposed reduction in ER Ca^{2+} concentration (Bassik et al., 2004; Foyouzi-Youssefi et al., 2000; Oakes et al., 2005; Palmer et al., 2004; Pinton et al., 2000; White et al., 2005), although a reduction in ER Ca^{2+} concentration has not been universally found and may not be necessary for Ca^{2+} signal regulation by Bcl-2/Bcl-X_L in all instances (Chen et al., 2004; Distelhorst and Shore, 2004; Hanson et al., 2008; Li et al., 2007).

To further understand Ca^{2+} regulation by Bcl-2/Bcl-X_L at a molecular level, recent studies focused on the interaction of Bcl-2 and Bcl-X_L with inositol 1,4,5-trisphosphate receptors (IP3R), based on coimmunoprecipitation from cell extracts (Chen et al., 2004; Hanson et al., 2008; Li et al., 2007; Oakes et al., 2005; White et al., 2005; Xu et al., 2007; Zhong et al., 2006). IP3-mediated Ca^{2+} efflux from the ER via IP3R Ca^{2+} channels generates Ca^{2+} signals mediating a wide range of cellular processes (Berridge et al., 2000), including apoptosis in response to T cell receptor (TCR) and B cell receptor activation, glucocorticosteroids, neurotoxic damage, oxidative stress, and Fas (Joseph and Hajnoczky, 2007). TCR engagement by antigen or by antibody to the CD3 component of the TCR complex activates phospholipase C, generating IP3, which induces Ca^{2+} release from the ER via IP3Rs (Lewis, 2001). Because of the critical roles played by TCR-mediated Ca^{2+} signals in both T cell survival and death (Gallo et al., 2006), a major focus of our work has been on the regulation of these Ca^{2+} signals by Bcl-2. We found that Bcl-2 inhibits both sustained Ca^{2+} elevation and apoptosis induced by strong TCR activation, while enhancing IP3-mediated Ca^{2+} oscillations induced by weak TCR activation (Chen et al., 2004; Zhong et al., 2006). In these studies, coimmunoprecipitation of Bcl-2 with IP3Rs and comigration of these proteins in blue native gels suggested that the regulatory effect of Bcl-2 on TCR-mediated Ca^{2+} signals is mediated through a Bcl-2-IP3R interaction that regulates IP3R channel opening.

The present work addresses three important questions regarding the regulation of IP3R channel activity by Bcl-2. First, does Bcl-2 at endogenous levels interact with IP3Rs and inhibit sustained TCR-mediated Ca^{2+} elevation? This is a critical question, since the inhibition of TCR-induced Ca^{2+} elevation was found in Bcl-2-negative WEHI7.2 T cells where Bcl-2 had been exogenously expressed (Chen et al., 2004; Zhong et al., 2006). Here we address this question by demonstrating that endogenous Bcl-2 in Jurkat cells, which is expressed at levels much lower than exogenously expressed Bcl-2, interacts with IP3Rs and that siRNA-mediated knockdown of Bcl-2 enhances TCR-mediated Ca^{2+} elevation. Second, does Bcl-2 interact with IP3Rs within intact living cells, or is the interaction previously demonstrated by coimmunoprecipitation only manifest in broken cell preparations? To address this, we demonstrate by two different Förster resonance energy transfer (FRET) methods that Bcl-2 and IP3Rs interact in intact cells. Third, is Bcl-2's inhibition of TCR-induced Ca^{2+} elevation and apoptosis mediated through Bcl-2 interaction with IP3Rs? To address this, we mapped a Bcl-2-interacting site on IP3Rs and thereby designed an inhibitory peptide that abrogates Bcl-2-IP3R interaction. This peptide not only reversed Bcl-2's inhibitory effect on IP3R channel opening in artificial lipid bilayers, but also reversed Bcl-2's inhibitory effect on TCR-induced Ca^{2+} elevation and apoptosis within cells, indicating that the interaction of Bcl-2 with IP3Rs contributes to Bcl-2's inhibitory effect on proapoptotic Ca^{2+} signals.

RESULTS

Bcl-2 Interacts with IP3R in Cells

FRET between Bcl-2 and IP3Rs was measured by acceptor photobleaching in fixed cells, which measures dequenching of donor (CFP) emission by acceptor (YFP) photobleaching (Hummer et al., 2003; Karpova et al., 2003; Li et al., 2005), and by three-cube FRET (two-color ratio imaging) in live cells (Erickson et al., 2001). In the first method, YFP-IP3R type 1 was used as acceptor and CFP-Bcl-2 was used as donor (Figure 1). Fluorophores were tagged to the cytoplasmic N terminus of both proteins (Figure 1B). When transiently expressed in COS-7 cells, using relatively low concentrations of expression vectors, CFPBcl-2 and YFP-IP3R were colocalized on the ER with a small fraction of CFP-Bcl-2 localized without YFP-IP3R to mitochondria (see Figure S1 available online). Regions where CFP and YFP colocalized were selected for FRET efficiency calculation; thus the calculated FRET efficiencies only represent the efficiencies in the regions where YFP fusions and CFP fusions colocalize, reducing the contribution from CFP on mitochondria. A cameleon Ca^{2+} sensor served as positive control (Miyawaki et al., 1997). CFP + YFP-IP3R, YFP + CFP-Bcl-2, and CFP + YFP were negative controls, along with CFP targeted to the cytoplasmic face of the ER (ER-CFP) + YFP-IP3R. ER-CFP localizes to the ER (Figure S1), serving as a negative control to exclude the possibility that FRET arising from the CFP-Bcl-2 and YFP-IP3R pair is merely due to the expression of fluorescently tagged proteins in the same location. After 30 min photobleaching with the YFP excitation fluorescence light, the CFP channel fluorescence intensity increased in both CFP-Bcl-2 + YFP-IP3R and CFP-YFP cameleon cells, but not in negative controls (Figure 1A). The CFP donor dequenching effect was clearly shown by subtracting prebleaching images from postbleaching images through pixel-by-pixel calculation (Figure 1A, CFP postbleach minus CFP prebleach). The CFP signal increased an average of 28% ± 1%in YFP-IP3R + CFP-Bcl-2 cells and 37% ± 0.6% in CFP-YFP cameleon cells following YFP bleaching (Figure 1C). The CFP fluorescence did not increase appreciably in negative control pairs.

To measure FRET in live cells, the same pairs of fluorescent proteins were transiently expressed in HEK293 cells (Figure S2). In live HEK293 cells, FRET occurs in CFP-YFP cameleon cells and CFP-Bcl-2 + YFP-IP3R cells, but not in control cells (Figure S2). These results, although less quantitative than those obtained with the acceptor photobleaching method (Piston and Kremers, 2007), indicate that FRET occurs, providing evidence that the Bcl-2-IP3R interaction exists not only in fixed cells, but also in living cells.

To summarize, taking into consideration technical limitations of FRET (see Discussion), measurements of FRET in both fixed and live cells indicate that Bcl-2 interacts with IP3Rs in intact cells, verifying the interaction predicted by coimmunoprecipitation of these proteins from cell extracts.

Endogenous Bcl-2 Interacts with IP3R and Inhibits TCR-Mediated Ca^{2+} Elevation

Jurkat cells were used to test if endogenous Bcl-2 interacts with IP3Rs and regulates TCR-mediated Ca^{2+} elevation. The level of endogenous Bcl-2 in Jurkat cells is much less than that of exogenously expressed Bcl-2 in WEHI7.2 cells [Bcl-2(+) WEHI7.2 cells] (Figure 2A). Nevertheless, Bcl-2 in Jurkat cells also coimmunoprecipitated with IP3Rs (Figure 2B), and siRNA-mediated knockdown of this Bcl-2 (Figure 2C) enhanced anti-CD3-induced Ca^{2+} elevation (Figures 2D and 2E), indicating the regulatory action of Jurkat cell Bcl-2 on IP3-mediated Ca^{2+} elevation. Also, siRNA-mediated knockdown of Bcl-2 in Jurkat cells did not alter thapsigargin-induced Ca^{2+} elevation (Figures 2F and 2G), suggesting that reducing the level of endogenous Bcl-2 did not affect ER Ca^{2+} concentration, a finding consistent

with earlier indirect and direct measurements of ER Ca^{2+} in Bcl-2- overexpressing WEHI7.2 cells (see Discussion).

To summarize, evidence that endogenous Bcl-2 in Jurkat T cells interacts with IP3Rs and regulates IP3-mediated Ca^{2+} elevation alleviates concern that the previously reported inhibition of TCR-induced Ca^{2+} elevation by Bcl-2 might be secondary to either clonal selection or high Bcl-2 levels associated with exogenous expression. Moreover, these findings enable investigation of both exogenously and endogenously expressed Bcl-2 throughout the experiments that follow.

Bcl-2 Interacts with the Regulatory and Coupling Domain of the IP3R

The three IP3R subtypes differ in terms of functional properties, expression patterns, and subcellular localization in different cell types (Bezprozvanny, 2005; Vermassen et al., 2004). Each IP3R monomer has a cytoplasmic region containing an IP3-binding and an inhibitory and coupling domain close to the N terminus and an internal regulatory and coupling domain between the IP3 binding and channel domains, while the C-terminal IP3R tail includes a gatekeeper domain (Figure 3A) (Taylor et al., 2004; Uchida et al., 2003).

To identify where Bcl-2 interacts on the IP3R, we used a series of GST-IP3R fusion constructs corresponding to five fragments covering the first N-terminal 2216 amino acids and 1 fragment corresponding to the last 160 amino acids of mouse IP3R type 1 (Figure 3A) (Lee et al., 2006). These fragments are located in the cytoplasm and coincide with “natural” domains generated by limited proteolysis (Yoshikawa et al., 1999). The transmembrane domain was not included. After purification, fragments migrated as single prominent bands corresponding to their expected molecular weights (Figures 3B and 3C), although some minor degradation products were detected.

The first set of GST pull-down experiments utilized extracts of Bcl-2(+) WEHI7.2 cells and Jurkat cells as two independent sources of Bcl-2. Cell extracts were incubated with GST-IP3R fragments prebound to glutathione sepharose resin, with equal loading of the GST-IP3R fragments (upper panels, Figures 3B and 3C). After pull-down, Bcl-2 bound to IP3R domains was detected by immunoblotting (lower panels, Figures 3B and 3C), indicating that Bcl-2 from each cellular source mainly interacted with IP3R domain 3. These experiments were repeated a total of five times with the same result. It is important to note that, following incubation of cell extracts with GST-IP3R fragments on the glutathione sepharose resin, the resin was washed extensively (see Experimental Procedures).

An interaction of Bcl-X_L with domain 6 of IP3R 1 was previously reported (White et al., 2005), but only three IP3R fragments were tested: an N-terminal fragment (aa 1–600); a C-terminal fragment (aa 2512–2750); and a larger fragment, Δ1–600, encompassing both the regulatory and coupling domain and the C terminus. Thus, on the basis of these mapping studies a potential interaction of Bcl-X_L/Bcl-2 within the regulatory and coupling domain was not formally tested. Also, the GST pull-down experiments employed stringency conditions lower than those in the present work. We therefore compared the interaction of Bcl-2 with domains 3 and 6 under three different buffer conditions, including the same buffer/wash conditions employed in our experiments described above (buffer 2), the buffer/wash condition employed by White et al. (2005) (buffer 1), and a buffer employing CHAPS detergent (buffer 3) rather than the nonionic detergents employed in the other two buffers (Figure 3D). The later control was included in view of earlier reports that nonionic detergents affect the Bcl-2 family member interactions (Hsu and Youle, 1997). With the lower stringency condition (buffer 1, 0.05% Triton, three times washing), domain 6 may interact with Bcl-2; however, under all three buffer conditions the interaction of domain 3 with Bcl-2 was much more prominent than the interaction of domain 6. Thus, it is possible

that Bcl-2 interacts with both of these IP3R regions, but because of the prominence of the interaction with domain 3, we choose to further analyze smaller fragments of domain 3, subdomains 3a (aa 1347–1496) and 3b (aa 1499–1649), to further narrow down the Bcl-2 binding region. These fragments correspond to smaller segments of the regulatory and coupling domain, as previously published (Sienaert et al., 1997) (Figure 3A). We found that Bcl-2 interacted with the 80 amino acid subdomain 3a1 (aa 1347–1426) most strongly (Figure 3E). Therefore, this subdomain was targeted to develop an inhibitory peptide, and experiments employing this peptide further confirm the contribution of subdomain 3a1 to the interaction between Bcl-2 and IP3R (below).

To address whether Bcl-2 associates with the IP3R directly or not, GST pull-down experiments were performed using purified His-tagged full-length Bcl-2 (Figure 3F). This protein retains its ability to bind Bim and Bax (Figure S3), as reported previously for GST-Bcl-2 (Bassik et al., 2004). Our findings, confirmed in three separate experiments, indicate that the purified His-tagged Bcl-2 also interacts with the GST-IP3R domain 3 fragment (Figure 3G). Thus, Bcl-2 directly interacts with the IP3R in vitro.

In preliminary experiments we found that deleting the BH4 domain from Bcl-2 prevented interaction of Bcl-2 with the IP3R (data not shown). We therefore screened a series of dicodon mutations in the BH4 domain and found that mutating amino acids 6 and 7 abrogated the Bcl-2-IP3R interaction (Figures S4A and S4B) and abrogated Bcl-2's inhibition of anti-CD3-induced calcium elevation (Figure S4C). These data indicate that the Bcl-2-IP3R interaction is necessary for Bcl-2's inhibitory effect on calcium, a conclusion that is further substantiated by the following evidence using an inhibitory peptide that prevents the Bcl-2-IP3R interaction.

An IP3R Peptide Inhibits Bcl-2-IP3R Interaction

Since the IP3R binding region was narrowed down to the 80 amino acid subdomain 3a1 (aa 1347–1426), we designed two 20 amino acid peptides (peptide 1, aa 1365–1384; peptide 2, aa 1389–1408) based on the degree of homology in this region among different IP3R isoforms (Figure 4A). Also, preference was given to regions that have beta-turn and/or α-helical structures, rather than random-coil or nonstructured sequences, expecting that one or both of the peptides could inhibit the Bcl-2-IP3R interaction. Furthermore, the C-terminal region of domain 3a1 was not selected because of its lower accessibility and unpredictable secondary structure (Invitrogen PeptideSelect Design Tool). The scrambled sequence of peptide 2 was also synthesized and used as a control (Figure 4A). The effect of the peptides on Bcl-2-IP3R interaction was initially tested in GST pull-down experiments using Bcl-2(+) WEHI7.2 extracts as a source of Bcl-2 (Figure 4B). Peptides (200 μM and 1 mM) were incubated with Bcl-2(+) WEHI7.2 cell extracts and GSTIP3R domain 3 attached to glutathione sepharose. The amount of bound Bcl-2 was significantly decreased by 200 μM or 1 mM peptide 2, but not by control peptide. At 1 mM, peptide 1 partially inhibited the interaction, but not as effectively as peptide 2. The inhibitory effect of peptide 2 on Bcl-2-IP3R interaction was also detected in coimmunoprecipitation assays employing both Bcl-2(+) WEHI7.2 cells (Figures 4C and 4D) and Jurkat cells (Figure 4E). Peptide 2 (400 μM) consistently inhibited Bcl-2-IP3R interaction, whereas control peptide and peptide 1 did not inhibit the interaction (Figures 4C–4E). These results were confirmed in multiple experiments. As a control for specificity, peptide 2 disrupted Bcl-2-IP3R interaction but not interaction of Bcl-2 with the BH3-only protein Bim (Figures 4F and 4G).

Peptide 2 Reverses Bcl-2's Inhibitory Effect on IP3R Channel Opening In Vitro

The effects of peptide 2 and purified Bcl-2 on IP3R channel activity were analyzed in planar lipid bilayers under steady-state conditions. Single IP3R type 1 channel activity was

visualized as a series of discrete positive current fluctuations in the presence of 2 μM IP3 and 250 nM Ca^{2+} in the *cis* compartment (cytoplasmic side of channel) (Figure 5A). A significant reduction in single channel activity was observed after adding 0.1 μM purified Bcl-2 to the cytoplasmic face of the IP3R channel (Figures 5A and 5B), and addition of 10 μM peptide 2 reversed Bcl-2's inhibitory effect on channel activity (Figure 5A). Average open probabilities under various conditions were calculated from multiple repeated experiments (Figure 5C). Addition of Bcl-2 reduced IP3R open probability by 11.5-fold to 0.018. Peptide 2 reversed Bcl-2's inhibitory effect, increasing the open probability back to 0.16, whereas control peptide did not reverse Bcl-2's inhibitory effect on channel activity (Figure 5C). These results demonstrate that peptide 2 reverses Bcl-2's inhibitory effect on IP3R channel opening in a purified in vitro system, indicating that peptide 2 acts directly on the Bcl-2-IP3R interaction to reverse Bcl-2's inhibitory effect on channel opening.

Peptide 2 Reverses Bcl-2's Inhibitory Effect on TCR-Induced Ca^{2+} Elevation

Next we investigated whether peptide 2 also reverses Bcl-2's inhibitory effect on Ca^{2+} release through the IP3R in Bcl-2(+) and (−) WEHI7.2 clones described previously (Chen et al., 2004), newly derived WEHI7.2 mixed populations exogenously expressing Bcl-2, and Jurkat cells. Optimal conditions for peptide delivery and anti-CD3 concentration were determined in preliminary experiments. Peptide delivery in the lipid bilayer is 100%, whereas the penetration of peptide 2 into cells is much less, accounting for the lesser effect in cells. Therefore, a higher concentration of peptide (60 μM) was delivered into cells using the Chariot delivery reagent. Cytoplasmic Ca^{2+} concentration was continuously measured at a single-cell level by digital imaging during anti-CD3 treatment. Representative Ca^{2+} traces from Bcl-2(+) WEHI7.2 cells are shown in Figure 6A, and the average Ca^{2+} elevation induced by anti-CD3 in seven experiments is summarized in Figure 6B. Observed variations in lag phase are at least partially attributable to the fact that lymphocytes are only loosely adherent to coverslips and thus rapid buffer exchange is not possible during antibody additions. Peptide 2 enhanced anti-CD3-induced Ca^{2+} elevation in Bcl-2(+) WEHI7.2 cells by 40%. Control peptide and peptide 1 did not enhance anti-CD3-induced Ca^{2+} elevation. In Bcl-2(−) cells, peptide 2 did not have a significant effect on Ca^{2+} (Figure 6B). Similarly, peptide 2 significantly enhanced anti-CD3-induced Ca^{2+} elevation in Jurkat cells, whereas control peptide and peptide 1 did not (Figures 6C and 6D). Peptide 2 had no effect on Ca^{2+} elevation when added to the cells in the absence of the Chariot reagent. Also, peptide 2 did not enhance anti-CD3-induced Ca^{2+} elevation in Jurkat cells where the endogenous Bcl-2 level had been knocked down by siRNA, further confirming that the effect of peptide 2 on Ca^{2+} is dependent upon its ability to disrupt the Bcl-2-IP3R interaction (Figure S5). Additionally, peptide 2 did not affect intracellular Ca^{2+} levels in the absence of anti-CD3 stimulation (data not shown). The low Bcl-2 level in Jurkat cells and the barely detectable endogenous Bcl-2 in Bcl-2(−) WEHI7.2 cells are consistent with the higher amplitude and longer duration of the Ca^{2+} response in these cells in contrast to Bcl-2(+) WEHI7.2 cells (compare Figures 6A and 6B to Figures 6C and 6D). Thus, peptide 2 modulated anti-CD3-induced Ca^{2+} elevation in both Bcl-2(+) WEHI7.2 cells and Jurkat cells, consistent with the ability of peptide 2 to disrupt Bcl-2-IP3R interaction.

To exclude the possibility that peptide 2 may interfere with the upstream TCR activation pathway, a cell-permeant IP3 ester (D-myo $InsP_3$ hexakisbutyryloxymethyl ester) was used to bypass TCR activation and anti-CD3-induced IP3 generation. Peptide 2 enhanced IP3 ester-induced Ca^{2+} elevation in Jurkat cells (Figures S6A and S6B), indicating that peptide 2 acts at the level of the IP3R rather than interfering with upstream components of the TCR signaling pathway.

The conclusion that peptide 2 acts directly on the Bcl-2-IP3R interaction is supported not only by experiments described above (Figure 5) in which peptide 2 reversed Bcl-2-mediated

inhibition of IP3R channel opening in vitro, but also by unidirectional $^{45}Ca^{2+}$ flux experiments (Figures S6D and S6E) that allow for very accurate quantification of Ca^{2+} release through IP3Rs located on the ER. These experiments require firmly adherent cells, and therefore murine embryonic fibroblasts (MEFs), which have a somewhat lower level of endogenous Bcl-2 than Jurkat cells (Figure S6C), were employed. The rate of IP3-induced $^{45}Ca^{2+}$ efflux was measured in the presence of thapsigargin, which completely prevents ER Ca^{2+} reuptake. Peptide 2, but not control peptide, significantly increased the rate of $^{45}Ca^{2+}$ efflux (Figures S6D and S6E), confirming that peptide 2 acts at the ER level to reverse Bcl-2's inhibition of IP3R activity.

Peptide 2 Enhances TCR-Induced Apoptosis

TCR-induced apoptosis is mediated by Ca^{2+} release from the ER via the IP3R, and as noted above, Bcl-2 inhibits TCR-induced apoptosis by inhibiting IP3-mediated Ca^{2+} release (Zhong et al., 2006). Since peptide 2 reverses Bcl-2's inhibitory effect on Ca^{2+} release, we next investigated whether peptide 2 also attenuates the inhibitory effect of Bcl-2 on anti-CD3-induced apoptosis. Peptides were delivered into Bcl-2(+) WEHI7.2 cells by Chariot reagent. After 3 hr, cells were treated with anti-CD3 antibody, and the percentage of apoptotic cells was measured 24 hr later. In Bcl-2(−) WEHI7.2 cells, anti-CD3 induced −18% apoptotic cells while the Bcl-2-overexpressing Bcl-2(+) WEHI7.2 cells display markedly inhibited anti-CD3-induced apoptosis (Figure 7B). Peptide 2 enhanced anti-CD3-induced apoptosis by 2-fold in Bcl-2(+) WEHI7.2 cells, whereas control peptide did not have a significant effect.

Peptide 2 also attenuated Bcl-2's inhibition of anti-CD3-induced apoptosis in Jurkat cells. In preliminary studies (data not shown), we tested several anti-CD3 concentrations. Higher concentrations of anti-CD3 induced high levels of apoptosis that might obscure the effect of the peptide. We therefore used 5 μg/ml anti-CD3, sufficient to induce 20%–30% apoptosis. Peptide 2 enhanced anti-CD3-induced apoptosis to 40%–45%, whereas the control peptide, peptide 1, or peptide 2 in the absence of Chariot reagent did not have an effect on anti-CD3-induced apoptosis (Figures 7A and 7C). In contrast to the effect of peptide 2 on anti-CD3-induced apoptosis, peptide 2 did not enhance Fas-induced Ca^{2+}-independent apoptosis in Jurkat cells (Figure S5B).

In summary, consistent with the effects of peptide 2 on the Bcl-2-IP3R interaction and on anti-CD3-induced Ca^{2+} elevation, peptide 2 enhanced anti-CD3-induced apoptosis in both Jurkat cells and Bcl-2(+) WEHI7.2 cells. In considering these findings, it is important keep in mind that Bcl-2 also inhibits apoptosis by binding to BH3-only proteins and that the effect of peptide 2 selectively interrupts Bcl-2-IP3R interaction, not the interaction of Bcl-2 with BH3-only proteins (see Figure 4F). Thus, it is to be expected that peptide 2 would only partially reverse Bcl-2's antiapoptotic activity.

DISCUSSION

Here we have used FRET measurements to document Bcl-2-IP3R interaction within intact cells and have mapped the site of Bcl-2 interaction on the IP3R, thereby developing an inhibitory peptide used to establish the importance of the Bcl-2-IP3R interaction in regulating Ca^{2+} signals. This peptide, referred to as peptide 2, corresponds to a 20 amino acid sequence in subdomain 3a1 of the IP3R, a sequence that displays a high degree of homology in all three IP3R isoforms. The GST-IP3R domains used to map the Bcl-2 binding region represent well-folded structural components retaining significant IP3-induced Ca^{2+} release activity in vitro as long as they remain assembled (Uchida et al., 2003; Yoshikawa et al., 1999). Thus, the interaction between Bcl-2 and subdomain 3a1 identified in our experiments likely corresponds to the interaction occurring in the natural situation. That this

IP3R subdomain is critical for the interaction of Bcl-2 with IP3Rs is substantiated by the ability of peptide 2 to inhibit this interaction in GST pull-down and coimmunoprecipitation experiments employing both Bcl-2(+) WEHI7.2 cells and endogenous Bcl-2-expressing Jurkat cells. Moreover, this action of peptide 2 in Jurkat cells is consistent with evidence, also presented here, that endogenously expressed Bcl-2 interacts with endogenously expressed IP3Rs. These findings alleviate concern that the Bcl-2-IP3R interaction might be dependent upon overexpression of Bcl-2 at high levels.

Domain 3a1, where Bcl-2 interacts, is located in the regulatory and coupling domain of the IP3R, which transfers the ligand binding signal from the N-terminal IP3 binding domain to the C-terminal channel domain. This domain also functions to keep the inactivated IP3R channel closed (Bezprozvanny, 2005; Nakayama et al., 2004; Szlufcik et al., 2006) and contains many target sites for regulators of IP3R activity (Patterson et al., 2004; Foskett et al., 2007). Moreover, recent electron microscopic findings suggested that conformational changes within the IP3R type 1 regulatory and coupling domain switch IP3R states between a “windmill”-like and “square”-like structure, which may represent the “open” and “closed” channel, respectively (Hamada et al., 2003; Serysheva et al., 2003; Taylor et al., 2004). Thus, it is interesting to speculate that the binding of Bcl-2 in this region may regulate this conformational change, thereby regulating IP3R channel opening.

The development of peptide 2 as an inhibitor of Bcl-2-IP3R interaction provided a useful tool with which to investigate the fundamental mechanism by which Bcl-2 inhibits Ca^{2+} release from the ER, at a molecular level. To this end, we employed peptide 2 in a multiplicity of experimental strategies to remove any doubt that the interaction of Bcl-2 with IP3Rs contributes to Bcl-2’s inhibition of IP3-mediated ER Ca^{2+} release. First, peptide 2 reversed Bcl-2’s inhibition of IP3R channel opening in vitro. Second, peptide 2, when introduced into cells using Chariot reagent, reversed Bcl-2’s inhibition of TCR-mediated Ca^{2+} elevation both in Bcl-2(+) WEHI7.2 cells and in Jurkat cells. These findings indicate that Bcl-2 inhibits proapoptotic Ca^{2+} signals at least in part through interaction with the IP3R. Third, special care was taken to control for the outside possibility that peptide 2 might act in cells at some other level than the IP3R itself (e.g., the TCR signaling pathway upstream of the IP3R). For this purpose, we demonstrated that peptide 2 antagonized both unidirectional $^{45}Ca^{2+}$ efflux from the ER in permeabilized cells and IP3 ester-induced Ca^{2+} elevation in intact cells. Thus, the present findings provide strong evidence that the Bcl-2-IP3R interaction is an important component of the process through which Bcl-2 inhibits IP3-mediated Ca^{2+} release from the ER.

One proposed component of this process upon which there is not complete agreement is the role of Bcl-2 in regulating ER Ca^{2+} concentration, a topic discussed in recent reviews (Distelhorst and Shore, 2004; Giacomello et al., 2007; Pinton and Rizzuto, 2006; Rong and Distelhorst, 2008). In our earlier work (Chen et al., 2004) and in the present study, as well as findings in other laboratories (see Introduction), a Bcl-2-imposed decrease in ER Ca^{2+} concentration was not detected. Nevertheless, the previously reported detection of a Bcl-2-imposed decrease in Ca^{2+} concentration by others and our present findings regarding the interaction of Bcl-2 with the IP3R are not necessarily mutually exclusive. In fact, recent reports propose a role for Bcl-2-IP3R interaction in regulating ER Ca^{2+} concentration (Oakes et al., 2005) and indicate that the ability of Bcl-2 to decrease ER Ca^{2+} concentration is dependent upon both Bcl-2 phosphorylation state (Bassik et al., 2004) and which of the three IP3R isoforms is expressed (Li et al., 2007). Overall, the major focus of the current work is not on reexamining potential effects of Bcl-2 on ER Ca^{2+} concentration, but on the Bcl-2-IP3R and designing a peptide inhibitor that reverses Bcl-2’s inhibitory effect on calcium release and apoptosis. These findings stand whether or not Bcl-2 decreases ER Ca^{2+} concentration.

That peptide 2, when introduced into intact cells, reverses Bcl-2's inhibition of TCR- or cell-permeable IP3 ester-induced Ca^{2+} elevation suggests that the Bcl-2-IP3R interaction previously detected by coimmunoprecipitation in cell extracts indeed occurs within intact cells. This conclusion is further substantiated by FRET measurements. Bcl-2 is known to localize to both the ER and mitochondria, but IP3Rs are mainly localized to the ER, and Bcl-2's inhibitory effect on IP3-mediated Ca^{2+} elevation is observed in cells where Bcl-2 is selectively targeted to the ER (Chen et al., 2004). The FRET measurements reported here document an interaction of Bcl-2 with IP3Rs on the ER, although FRET techniques are challenging and have recognized pitfalls and limitations (Piston and Kremers, 2007). Therefore, in this work we employed two different, independent methods of FRET measurement, acceptor photobleaching in fixed cells and direct FRET measurements in living cells, as complementary methods to determine if Bcl-2 interacts with IP3R in cells. Also, because of the known limitations of both of these methods, a stringent set of controls was included. The most straightforward method to detect FRET is to photobleach the acceptor and to monitor the change in donor emission. For this method the actual FRET signal and the FRET efficiency could be overestimated depending on conditions (e.g., fixation) used (Rizzo et al., 2006). Thus, the quantification of FRET efficiencies in acceptor photobleaching experiments at present is valid only for establishing the presence or absence of FRET (Karpova et al., 2003). A number of negative controls reduced the possibility of false-positive FRET. Although live cell FRET by ratiometric imaging is the simplest FRET method, potential artifacts due to the spectral bleed-through have to be considered. The corrective ratiometric method employed in our measurements of live cell FRET has been established to subtract the crosstalk between the fluorescence proteins (see appendix of Erickson et al., 2001). Though actual FRET values depend on the exact amount of acceptor proteins interacting with donor proteins, it is not necessary for the donor and acceptor concentrations to be equal in both of the methods employed here (Erickson et al., 2001; Piston and Kremers, 2007). Nevertheless, according to the experimental conditions, the CFP-Bcl-2 and YFP-IP3R concentrations do not vary dramatically. Our data indicate that donor and acceptor pairs interact in sufficiently close proximity and orientation to allow FRET. With these precautions in mind, both FRET techniques provided positive evidence that Bcl-2 does indeed interact with IP3Rs within cells.

Overall, the findings presented here indicate that Bcl-2 operates on two fronts, blocking BH3-only protein activity and blocking proapoptotic Ca^{2+} signals. Recently developed Bcl-2 antagonists target the Bcl-2-BH3-only protein interaction, whereas peptide 2 interferes selectively with the Bcl-2-IP3R interaction. Perhaps in the future small-molecule inhibitors of the latter interaction could be developed that mimic the activity of peptide 2 and complement the therapeutic activity of small compounds targeting the interaction of Bcl-2 with BH3-only proteins.

EXPERIMENTAL PROCEDURES

Reagents

Fura-2 AM and Hoechst 33342 were from Invitrogen. Hamster anti-mouse CD3e ε chain mAb and mouse anti-hamster IgG1 were from BD Biosciences. Mouse anti-human CD3e IgG was purchased from eBioscience. D-myo-IP3 ester was synthesized by S.J. Conway, University of St. Andrews (Conway et al., 2006).

Plasmids

IP3R fragments were fused with GST at their N terminus and cloned into pGEX-6p2 vectors as described (Lee et al., 2006; Sienaert et al., 1997). Other plasmids and their source are as

follows: pECFP-Bcl-2, J. Yuan; CFP-YFP cameleon, R. Tsien; Bcl-2 mutants, T. Parslow; ER-CFP (SRbeta-mCerulean), F. Geng and D. Andrews.

Cell Culture and Transfection

COS-7 cells and WEHI7.2 cells (wild-type WEHI7.2, Bcl-2-overexpressing WEHI7.2 [Bcl-2(+) WEHI7.2], and WEHI7.2 cells transfected with empty vector [Bcl-2(−) WEHI7.2]) were cultured as described (Chen et al., 2004). Jurkat cells were cultured in RPMI1640 supplemented with 10% fetal bovine serum. Transfection in COS-7 cells was performed with FuGENE 6 from Roche. Transfection and cloning of Bcl-2 in WEHI7.2 cells were reported previously (Chen et al., 2004).

FRET

Plasmids encoding combinations of CFP- and YFP-tagged proteins were transiently transfected into COS-7 cells or HEK293 cells. For acceptor photobleaching FRET, COS-7 cells were fixed in 4% paraformaldehyde for 10 min after 24 hr transfection. Each FRET pair sample was measured by acceptor photobleaching and modified three-cube FRET method (see Supplemental Data).

Protein Expression and GST Pull-Down

GST-IP3R fragments were expressed and purified as described (Lee et al., 2006; Sienaert et al., 1997). WEHI7.2 cells were lysed with RIPA buffer (50 mM Tris-HCl, 150 mM NaCl, 1 mM EDTA, 1% NP-40, 0.5% sodium deoxycholate, 1 mM NaF, 1 mM Na_3PO_4, and protease inhibitor cocktail [Roche]). Supernatant (250 μl), which contained 300 μg total protein, was precleared with 25 μl sepharose beads (Amersham Biosciences) for 1 hr and then pelleted to remove the beads. Ten to twenty micrograms of each GST-IP3R fragment was attached to a fresh batch of 25 μl sepharose beads and incubated with the precleared cell supernatant for 1 hr at 4°C. The amounts of each GST-IP3R fragment used in pull-down assays were adjusted to similar levels. To reduce nonspecific binding, 1% BSA was added to the pull-down reaction, and NaCl concentration was adjusted to 300 mM during the binding step. Beads were centrifuged, washed thoroughly seven to eight times with RIPA buffer, eluted with glutathione elution buffer, and prepared for western blotting.

In certain experiments, three different buffer and wash conditions of differing stringencies were compared. The buffer/wash condition described above is termed buffer 2, and the same buffer/wash, except for replacement of the 1% NP40 with 1% CHAPS, is referred to as buffer 3. The buffer 1 buffer/ wash condition, which was employed previously in the work of White et al. (2005), consists of PBS, 2% glycerol, 0.05% Triton, and protease inhibitor cocktail. This buffer was used, without adding BSA or additional NaCl, for preparation of cell lysates, bead binding, and three-time washes.

Full-length Bcl-2 with His tag was cloned into pPROEX-1 vector and expressed in *E. coli* M15 cells. Ni-NTA spin (QIAGEN) was used to purify the His-Bcl-2 protein using the method described previously (Lam et al., 1998). Eluted Bcl-2 protein was further dialyzed to remove traces of CHAPS and imidazole, then characterized by SDS-PAGE, followed by silver staining and western blotting.

Immunoprecipitation and Western Blotting

Coimmunoprecipitation methods were described previously (Chen et al., 2004). The following antibodies were used: anti-human Bcl-2 (BD Biosciences), anti-mouse Bcl-2 (Santa Cruz Biotechnology), anti-IP3R type 1 (Calbiochem), anti-Bim (Sigma), anti-Bax (BD PharMingen), anti-GST (Amersham Biosciences), and anti-actin (Sigma). In the peptide inhibition of immunoprecipitation experiments, 10^8 cells were lysed with 500 μl

lysis buffer. The supernatant of cell lysates was incubated with the peptides at 4°C for 30 min before the immunoprecipitation.

Peptide Synthesis and Delivery

The purity of synthesized peptides was >95%, verified by mass spectrometry and HPLC. Each peptide was delivered into cells by Chariot (Active Motif) reagent according to manufacturer instructions. Peptides were mixed with Chariot reagent, incubated for 30 min at 25°C, and then added to suspensions of 10^6 cells in OPTI-MEM (Invitrogen) with the peptide concentration at 60 μM. After 30 min incubation, another 1.6 ml culture medium was added into the dish, diluting the peptide final concentration to −20 μM. Cells were incubated for another 2–3 hr in 5% CO_2 at 37°C before Ca^{2+} measurements.

Planar Lipid Bilayer Analysis of IP3R Channel Activity

Microsomes for use in bilayer experiments were prepared as described previously (Bare et al., 2005). Detailed methods for bilayer experiments are provided in the Supplemental Data.

Ca^{2+} Imaging and Fluorometric Measurements

Anti-mouse CD3, anti-human CD3 antibodies (20 μg/ml), or IP3 ester (25 μM) was gently added to buffer overlaying poly-L-Lysine-coated coverslips on which cells were adhered and loaded with Fura-2 AM. Methods of Ca^{2+} imaging and Ca^{2+} measurements by fluorometry were described in detail previously (Chen et al., 2004; Zhong et al., 2006).

RNA Interference

Jurkat cells were electroporated in a BioRad Gene Pulser with either a nontargeting smartpool or a human Bcl-2 smartpool from Dharmacon at a final concentration of 1 mM. Samples were then taken for western blotting at 0, 24, 48, and 72 hr after transfection, and 3×10^5 cells were plated onto poly-L-lysine-coated coverslips at each time point to measure Ca^{2+}. Cells were split every 24 hr to ensure optimal growth conditions.

Anti-CD3-Induced Apoptosis

After 24 hr treatment with 5 μg/ml anti-human CD3 for Jurkat cells and 20 μg/ml hamster anti-mouse CD3 plus anti-hamster IgG for WEHI7.2 cells, cells were stained with 10 μg/ml Hoechst 33342 for 10 min and typical apoptotic nuclear morphology was detected by epifluorescence microscopy with a 40× objective as previously described (Zhong et al., 2006).

Statistical Analysis

Data were summarized as the mean ± SEM, and comparisons were made using the two-tailed Student's t test for repeated measures. Differences between means were accepted as statistically significant at the 95% level ($p < 0.05$).

Supplementary Material

Refer to Web version on PubMed Central for supplementary material.

Acknowledgments

We thank Roger Tsien, Junying Yuan, Tristram Parslow, Fei Geng, David Andrews, and Stuart J. Conway for plasmids and reagents. We thank Susann Brady-Kalnay, Anthony Berdis, George Dubyak, and William Schilling for helpful discussions. We also thank Minh Lam, Cancer Center imaging core, for confocal microscopy. This work was supported by NIH grants CA085804 and CA42755 (C.W.D.) and HL80101 and MH53367 (G.A.M.), by

Research Programme G.0604.07 of the Research Foundation-Flanders (to H.D.S. and J.B.P.), and by Royal Society fellowship (to H.L.R.). G.B. is a Postdoctoral Fellow of the Research Foundation-Flanders.

References

Bare DJ, Kettlun CS, Liang M, Bers DM, Mignery GA. Cardiac type 2 inositol 1,4,5-trisphosphate receptor: interaction and modulation by calcium/calmodulin-dependent protein kinase II. J Biol Chem. 2005; 280:15912–15920. [PubMed: 15710625]

Bassik MC, Scorrano L, Oakes SA, Pozzan T, Korsmeyer SJ. Phosphorylation of Bcl-2 regulates ER Ca2+ homeostasis and apoptosis. EMBO J. 2004; 23:1207–1216. [PubMed: 15010700]

Berridge MJ, Lipp P, Bootman MD. The versatility and universality of calcium signalling. Nat Rev Mol Cell Biol. 2000; 1:11–21. [PubMed: 11413485]

Bezprozvanny I. The inositol 1,4,5-trisphosphate receptors. Cell Calcium. 2005; 38:261–272. [PubMed: 16102823]

Chen R, Valencia I, Zhong F, McColl KS, Roderick HL, Bootman MD, Berridge MJ, Conway SJ, Holmes AB, Mignery GA, et al. Bcl-2 functionally interacts with inositol 1,4,5-trisphosphate receptors to regulate calcium release from the ER. J Cell Biol. 2004; 166:193–203. [PubMed: 15263017]

Conway SJ, Thuring JW, Andreu S, Kvinlaug BT, Roderick HL, Bootman MD, Holmes AB. The synthesis of membrane permeant derivatives of myo-inositol 1,4,5-trisphosphate. J Chem. 2006; 59:887–893.

Cory S, Adams JM. The Bcl-2 family: regulators of the cellular life-or-death switch. Nat Rev Cancer. 2002; 2:647–656. [PubMed: 12209154]

Danial NN, Korsmeyer SJ. Cell death: critical control points. Cell. 2004; 116:205–219. [PubMed: 14744432]

Distelhorst CW, Shore GC. Bcl-2 and calcium: controversy beneath the surface. Oncogene. 2004; 23:2875–2880. [PubMed: 15077150]

Erickson MG, Alseikhan BA, Peterson BZ, Yue DT. Preassociation of calmodulin with voltage-gated Ca^{2+} channels revealed by FRET in single living cells. Neuron. 2001; 31:973–985. [PubMed: 11580897]

Foskett JK, White C, Cheung KH, Mak DO. Inositol trisphosphate receptor Ca^{2+} release channels. Physiol Rev. 2007; 87:593–658. [PubMed: 17429043]

Foyouzi-Youssefi R, Arnaudeau S, Borner C, Kelley WL, Tschopp J, Lew DP, Demaurex N, Krause KH. Bcl-2 decreases the free Ca^{2+} concentration within the endoplasmic reticulum. Proc Natl Acad Sci USA. 2000; 97:5723–5728. [PubMed: 10823933]

Gallo EM, Cante-Barrett K, Crabtree GR. Lymphocyte calcium signaling from membrane to nucleus. Nat Immunol. 2006; 7:25–32. [PubMed: 16357855]

Giacomello M, Drago I, Pizzo P, Pozzan T. Mitochondrial Ca^{2+} as a key regulator of cell life and death. Cell Death Differ. 2007; 14:1267–1274. [PubMed: 17431419]

Hamada K, Terauchi A, Mikoshiba K. Three-dimensional rearrangements within inositol 1,4,5-trisphosphate receptor by calcium. J Biol Chem. 2003; 278:52881–52889. [PubMed: 14593123]

Hanson CJ, Bootman MD, Roderick HL. Cell signaling: IP3 receptors channel calcium into cell death. Curr Biol. 2004; 14:R933–R935. [PubMed: 15530388]

Hanson CJ, Bootman MD, Distelhorst CW, Wojcikiewicz RJ, Roderick HL. Bcl-2 suppresses Ca(2+) release through inositol 1,4,5-trisphosphate receptors and inhibits Ca(2+) uptake by mitochondria without affecting ER calcium store content. Cell Calcium. 2008 Published online April 11, 2008. 10.1016/j.ceca.2008.01.003

Hsu YT, Youle RJ. Nonionic detergents induce dimerization among members of the Bcl-2 family. J Biol Chem. 1997; 272:13829–13834. [PubMed: 9153240]

Hummer A, Delzeith O, Gomez SR, Moreno RL, Mark MD, Herlitze S. Competitive and synergistic interactions of G protein β2 and Ca^{2+} channel β1b subunits with Cav2.1 channels, revealed by mammalian two-hybrid and fluorescence resonance energy transfer. J Biol Chem. 2003; 278:49386–49400. [PubMed: 14507926]

Joseph SK, Hajnoczky G. IP(3) receptors in cell survival and apoptosis: Ca(2+) release and beyond. Apoptosis. 2007; 12:951–968. [PubMed: 17294082]

Karpova TS, Baumann CT, He L, Wu X, Grammer A, Lipsky P, Hager GL, McNally JG. Fluorescence resonance energy transfer from cyan to yellow fluorescent protein detected by acceptor photobleaching using confocal microscopy and a single laser. J Microsc. 2003; 209:56–70. [PubMed: 12535185]

Lam M, Bhat MB, Nunez G, Ma J, Distelhorst CW. Regulation of Bcl-xL channel activity by calcium. J Biol Chem. 1998; 273:17307–17310. [PubMed: 9651311]

Lee B, Vermassen E, Yoon SY, Vanderheyden V, Ito J, Alfandari D, De Smedt H, Parys JB, Fissore RA. Phosphorylation of IP3R1 and the regulation of [Ca2+]i responses at fertilization: a role for the MAP kinase pathway. Development. 2006; 133:4355–4365. [PubMed: 17038520]

Lewis RS. Calcium signaling mechanisms in T lymphocytes. Annu Rev Immunol. 2001; 19:497–521. [PubMed: 11244045]

Li X, Hummer A, Han J, Xie M, Melnik-Martinez K, Moreno RL, Buck M, Mark MD, Herlitze S. G protein beta2 subunit-derived peptides for inhibition and induction of G protein pathways. Examination of voltage-gated Ca^{2+} and G protein inwardly rectifying K+ channels. J Biol Chem. 2005; 280:23945–23959. [PubMed: 15824105]

Li C, Wang X, Vais H, Thompson CB, Foskett JK, White C. Apoptosis regulation by Bcl-x(L) modulation of mammalian inositol 1,4,5-trisphosphate receptor channel isoform gating. Proc Natl Acad Sci USA. 2007; 104:12565–12570. [PubMed: 17636122]

Miyawaki A, Llopis J, Heim R, McCaffery JM, Adams JA, Ikura M, Tsien RY. Fluorescent indicators for Ca^{2+} based on green fluorescent proteins and calmodulin. Nature. 1997; 388:882–887. [PubMed: 9278050]

Nakayama T, Hattori M, Uchida K, Nakamura T, Tateishi Y, Bannai H, Iwai M, Michikawa T, Inoue T, Mikoshiba K. The regulatory domain of the inositol 1,4,5-trisphosphate receptor is necessary to keep the channel domain closed: possible physiological significance of specific cleavage by caspase 3. Biochem J. 2004; 377:299–307. [PubMed: 12968951]

Oakes SA, Scorrano L, Opferman JT, Bassik MC, Nishino M, Pozzan T, Korsmeyer SJ. Proapoptotic BAX and BAK regulate the type 1 inositol trisphosphate receptor and calcium leak from the endoplasmic reticulum. Proc Natl Acad Sci USA. 2005; 102:105–110. [PubMed: 15613488]

Orrenius S, Zhivotovsky B, Nicotera P. Regulation of cell death: The calcium-apoptosis link. Nat Rev Mol Cell Biol. 2003; 4:552–565. [PubMed: 12838338]

Palmer AE, Jin C, Reed JC, Tsien RY. Bcl-2-mediated alterations in endoplasmic reticulum Ca^{2+} analyzed with an improved genetically encoded fluorescent sensor. Proc Natl Acad Sci USA. 2004; 101:17404–17409. [PubMed: 15585581]

Patterson RL, Boehning D, Snyder SH. Inositol 1,4,5-trisphosphate receptors as signal integrators. Annu Rev Biochem. 2004; 73:437–465. [PubMed: 15189149]

Pinton P, Ferrari D, Magalhaes P, Schulze-Osthoff K, Di Virgilio F, Pozzan T, Rizzuto R. Reduced loading of intracellular Ca^{2+} stores and downregulation of capacitative Ca^{2+} influx in Bcl-2 overexpressing cells. J Cell Biol. 2000; 148:857–862. [PubMed: 10704437]

Pinton P, Rizzuto R. Bcl-2 and Ca^{2+} homeostasis in the endoplasmic reticulum. Cell Death Differ. 2006; 13:1409–1418. [PubMed: 16729032]

Piston DW, Kremers GJ. Fluorescent protein FRET: the good, the bad and the ugly. Trends Biochem Sci. 2007; 32:407–414. [PubMed: 17764955]

Rizzo MA, Springer G, Segawa K, Zipfel WR, Piston DW. Optimization of pairings and detection conditions for measurement of FRET between cyan and yellow fluorescent proteins. Microsc Microanal. 2006; 12:238–254. [PubMed: 17481360]

Rong Y, Distelhorst CW. Bcl-2 protein family members: versatile regulators of calcium signaling in cell survival and apoptosis. Annu Rev Physiol. 2008; 70:73–91. [PubMed: 17680735]

Serysheva II, Bare DJ, Ludtke SJ, Kettlun CS, Chiu W, Mignery GA. Structure of the type 1 inositol 1,4,5-trisphosphate receptor revealed by electron cryomicroscopy. J Biol Chem. 2003; 278:21319–21322. [PubMed: 12714606]

Sienaert I, Missiaen L, De Smedt H, Parys JB, Sipma H, Casteels R. Molecular and functional evidence for multiple Ca^{2+}-binding domains in the type 1 inositol 1,4,5-trisphosphate receptor. J Biol Chem. 1997; 272:25899–25906. [PubMed: 9325322]

Szlufcik K, Missiaen L, Parys JB, Callewaert G, De Smedt H. Uncoupled IP3 receptor can function as a Ca^{2+}-leak channel: cell biological and pathological consequences. Biol Cell. 2006; 98:1–14. [PubMed: 16354157]

Taylor CW, da Fonseca PC, Morris EP. IP(3) receptors: the search for structure. Trends Biochem Sci. 2004; 29:210–219. [PubMed: 15082315]

Uchida K, Miyauchi H, Furuichi T, Michikawa T, Mikoshiba K. Critical regions for activation gating of the inositol 1,4,5-trisphosphate receptor. J Biol Chem. 2003; 278:16551–16560. [PubMed: 12621039]

Vermassen E, Parys JB, Mauger JP. Subcellular distribution of the inositol 1,4,5-trisphosphate receptors: functional relevance and molecular determinants. Biol Cell. 2004; 96:3–17. [PubMed: 15093123]

White C, Li C, Yang J, Petrenko NB, Madesh M, Thompson CB, Foskett JK. The endoplasmic reticulum gateway to apoptosis by Bcl-Xl modulation of the InsP3R. Nat Cell Biol. 2005; 7:1021–1028. [PubMed: 16179951]

Xu L, Kong D, Zhu L, Zhu W, Andrews DW, Kuo TH. Suppression of IP3-mediated calcium release and apoptosis by Bcl-2 involves the participation of protein phosphatase 1. Mol Cell Biochem. 2007; 295:153–165. [PubMed: 16874461]

Yoshikawa F, Iwasaki H, Michikawa T, Furuichi T, Mikoshiba K. Trypsinized cerebellar inositol 1,4,5-trisphosphate receptor. Structural and functional coupling of cleaved ligand binding and channel domains. J Biol Chem. 1999; 274:316–327. [PubMed: 9867846]

Zhong F, Davis MC, McColl KS, Distelhorst CW. Bcl-2 differentially regulates Ca^{2+} signals according to the strength of T cell receptor activation. J Cell Biol. 2006; 172:127–137. [PubMed: 16391001]

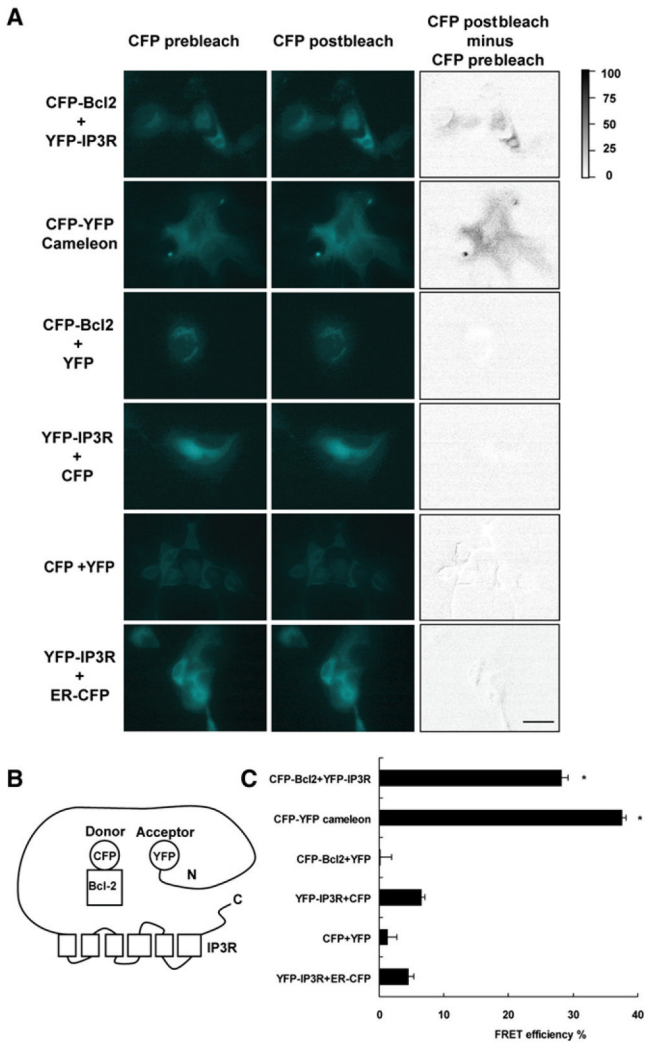

Figure 1. FRET Detection of Bcl-2-IP3R Interaction

FRET was detected by the increase of CFP fluorescence following YFP bleaching in COS-7 cells expressing CFP-Bcl-2 + YFP-IP3R and CFP-YFP cameleon, but not control combinations of fluorescently tagged proteins.

(A) Representative images of CFP fluorescence intensity before and after YFP photobleaching (left and middle columns). Gray value images (right column) were obtained by pixel-by-pixel subtraction of CFP prebleach images from postbleach images, with relative intensity differences represented by the gray scale. Scale bar, 5 μm.

(B) Diagram of C-terminal location of CFP and YFP on Bcl-2 and IP3R, respectively.

(C) Multiple regions of interest (>60 for each pair of samples) were randomly selected from the CFP and YFP colocalization regions in three individual experiments. FRET efficiency was calculated according to the increase in CFP emission by Volocity software. Symbols represent mean ± SEM. *$p < 0.01$.

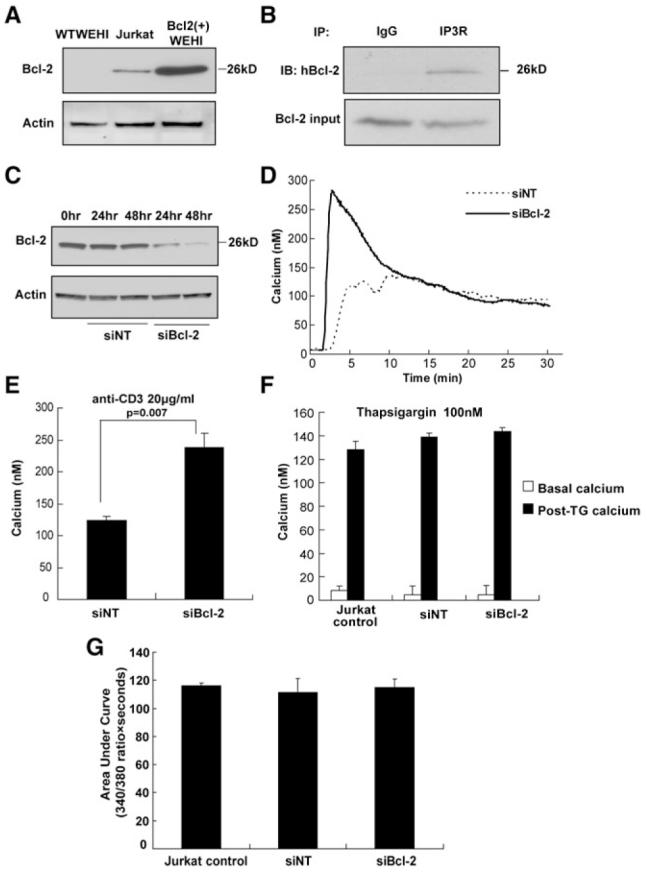

Figure 2. Endogenous Bcl-2 Inhibits Anti-CD3-Induced Ca^{2+} Elevation in Jurkat Cells

(A) Bcl-2 levels in wild-type WEHI7.2, Jurkat, and Bcl-2(+) WEHI7.2 cells by immunoblotting.

(B) Coimmunoprecipitation of Bcl-2 with IP3R in Jurkat extracts; immunoblot analysis using anti-Bcl-2 antibody.

(C) Immunoblot of Bcl-2 in Jurkat extracts 24 and 48 hr after transfection with nontargeting control siRNA (siNT) or Bcl-2 siRNA (siBcl-2).

(D) Digital imaging traces (average 160 cells per sample) monitoring Ca^{2+} elevation induced by 20 μg/ml anti-CD3 in the presence of extracellular Ca^{2+}.

(E) Peak Ca^{2+} elevation induced by 20 μg/ml anti-CD3 in presence of extracellular Ca^{2+} (mean ± SEM, three experiments).

(F) Peak Ca^{2+} elevation induced by 100 nM thapsigargin, measured fluorometrically in the absence of extracellular Ca^{2+} (mean ± SEM, three experiments).

(G) Area under the cytosolic Ca^{2+} 340 nM/380 nM ratio curve in (F) (mean ± SEM, three experiments).

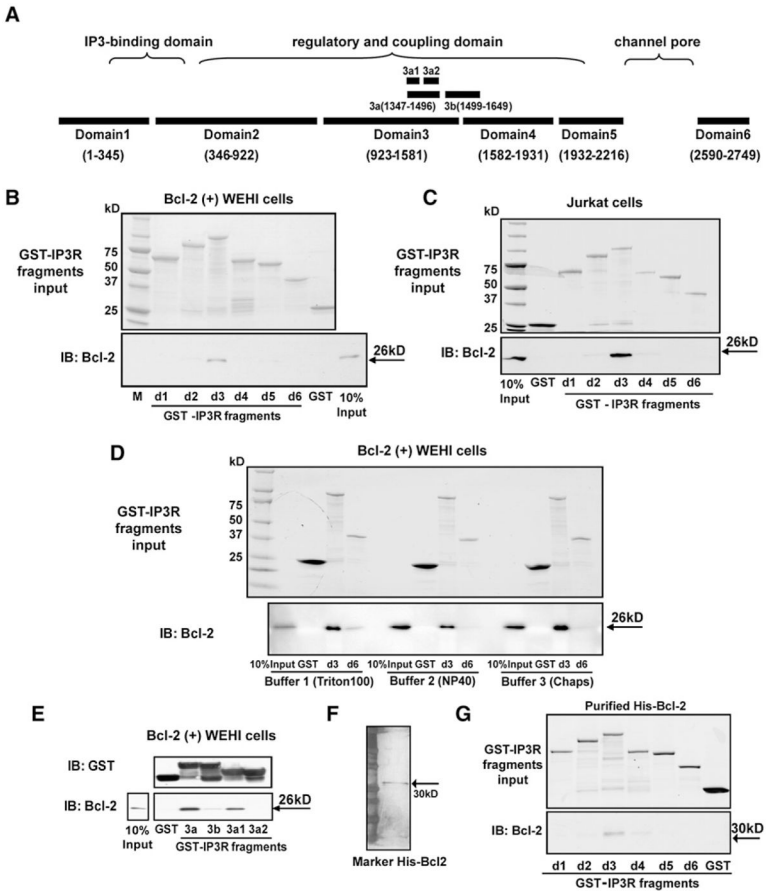

Figure 3. Bcl-2-IP3R Interaction Mapping

(A) Diagram of type 1 IP3R domains.

(B and C) GST-IP3R fragment pull-downs employing cytosolic extracts from Bcl-2(+) WEHI7.2 or Jurkat cells as Bcl-2 source. (Upper panel) Coomassie blue-stained gel showing input GST-IP3R fragments; (bottom panel) Bcl-2 detected by immunoblotting. Findings representative of five experiments using Bcl-2(+) WEHI7.2 extract and two experiments using Jurkat extract indicate that Bcl-2 mainly interacts with domain 3.

(D) Cell extracts from Bcl-2(+) WEHI7.2 cells were prepared in three different buffers, which differ mainly by detergent type and concentration. The same buffers were used during GST-IP3R pull-down and wash steps, except that in buffers 2 and 3 1% BSA was added and the NaCl concentration was increased to 300 mM in the binding steps to increase binding specificity. Also, wash steps were repeated three times with buffer 1, but seven to eight times with buffers 2 and 3. (Upper panel) Coomassie blue staining of GST-IP3R fragments, repeated twice with the same result.

(E) GST pull-down, performed as in (B), using GSTIP3R subdomain fragments 3a, 3b, 3a1, and 3a2. (Upper panel) Anti-GST immunoblot documenting input levels of IP3R fragments. (Lower panel) Anti-Bcl-2 immunoblot documenting that subdomain 3a1 is the major binding region of Bcl-2 on the IP3R. This experiment was repeated twice with the same result.

(F) Silver-stain gel indicating the purity of His-tagged Bcl-2.

(G) GST pull-down with purified His-tagged Bcl-2. (Upper panel) Input GST-IP3R fragments resolved by SDS-PAGE and stained with Coomassie blue. (Bottom panel)

Immunoblot for Bcl-2 showing that purified 30 kDa His-Bcl-2 directly interacted with GST-IP3R domain 3, repeated three times with the same result.

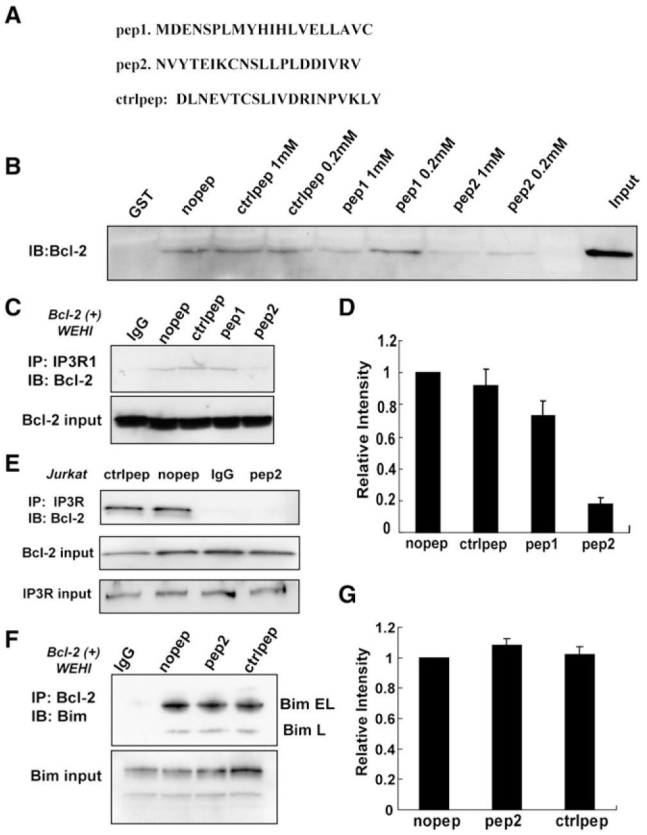

Figure 4. An IP3R Peptide Inhibits Bcl-2-IP3R Interaction but Not Bim-Bcl-2 Interaction

(A) Sequences of peptides 1 and 2, corresponding to regions within IP3R subdomain 3a1, and control peptide representing a scrambled sequence of peptide 2. (B) Peptide 2 inhibits the interaction between Bcl-2 and GST-IP3R domain 3 in GST pull-down assays. Bcl-2(+) WEHI7.2 cell extracts were preincubated with 200 μM or 1 mM peptides for 20 min before adding the glutathione sepharose resin with GST-IP3R domain 3 fragment attached. (C and E) IP3R was immunoprecipitated from extracts of Bcl-2(+) WEHI7.2 cells (C) or Jurkat cells (E) in the presence of 400 μM peptides. Peptide 2, but not peptide 1 or control peptide, inhibited the Bcl-2-IP3R coimmunoprecipitation. (D) Summary of Bcl-2 immunoblot signal intensities in three GST pull-down experiments identical to (C) (mean ± SEM). (F) Bcl-2 was immunoprecipitated from Bcl-2(+) WEHI7.2 cell extracts in the presence of 400 μM peptides, and coimmunoprecipitation of Bim was detected by anti-Bim immunoblotting. Neither control peptide nor peptide 2 interfered with the Bcl-2-Bim interaction. (G) Summary of Bim immunoblot signal intensities in three experiments identical to (F) (mean ± SEM).

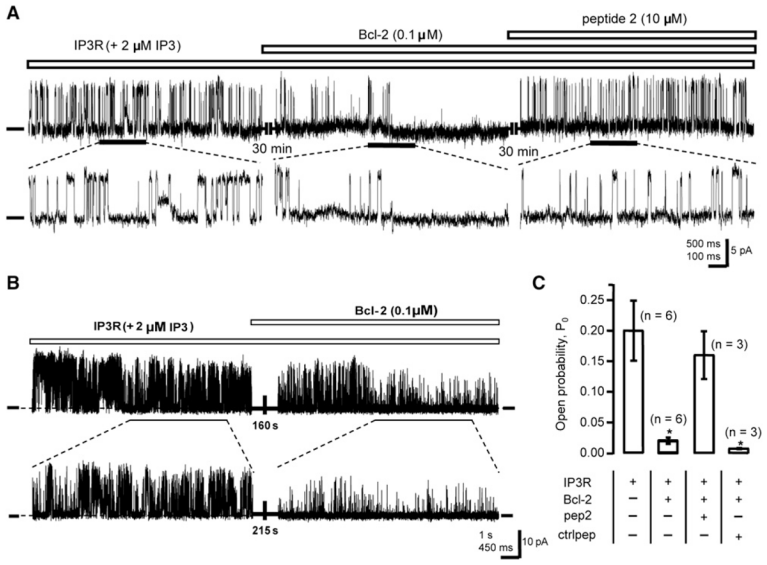

Figure 5. Peptide 2 Reverses Bcl-2's Inhibition of IP3R Channel Opening In Vitro

(A) IP3R type 1 single channel recordings at 0 mV in planar lipid bilayers with 250 nM Ca^{2+} and 2 μM IP3 in the *cis* (cytosolic) compartment (zero-current level marked). Current traces at the expanded time scale are shown in the bottom panel. Purified Bcl-2 (0.1 μM), added to the *cis* compartment, blocked channel activity. Subsequent addition of peptide 2 (10 μM) reversed Bcl-2's inhibition of channel activity.

(B) Shown is a single channel recording documenting that significant reduction of channel activity is detected within less than 3 min after Bcl-2 addition.

(C) Summary of multiple experiments (mean ± SEM) measuring effects of Bcl-2 and peptides on IP3R channel open probability. n = number of individual channels examined. Symbols represent mean ± SEM. *$p < 0.05$.

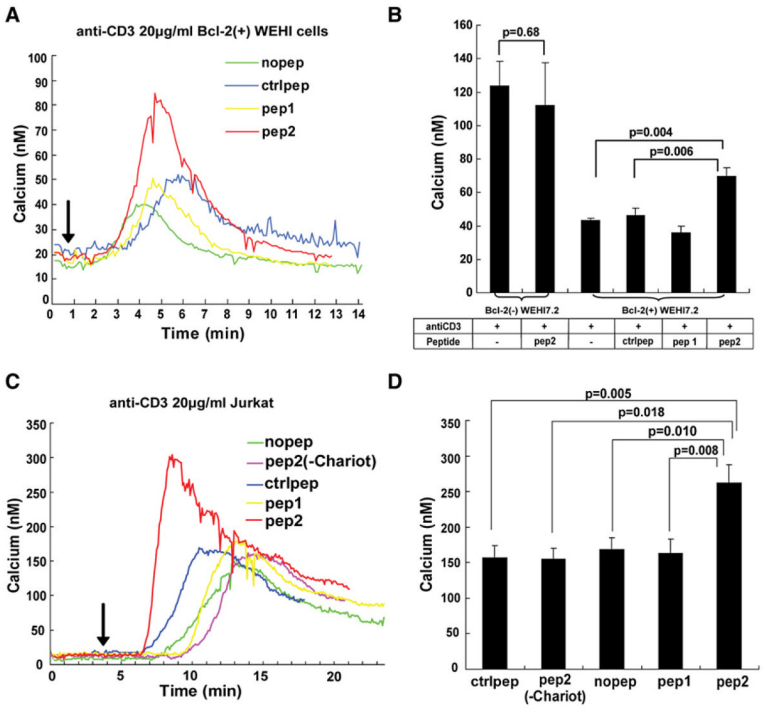

Figure 6. Peptide 2 Reverses Bcl-2's Inhibition of Anti-CD3-Induced Ca^{2+} Elevation

(A) Representative Ca^{2+} traces (each the mean of −65 cells) recording anti-CD3 (arrow, time of addition)- induced Ca^{2+} elevation in Bcl-2(+) WEHI7.2 cells. Peptide (60 μM) uptake was facilitated by Chariot reagent.

(B) Peak anti-CD3 induced Ca^{2+} elevation in Bcl-2(−) and Bcl-2(+) WEHI7.2 cells treated with peptides as in (A) [mean ± SEM, five experiments for Bcl-2(−) and seven experiments for Bcl-2(+) cells, with mean 68 cells per sample per experiment].

(C) Representative Ca^{2+} traces in Jurkat cells (mean 85 cells each). Treatment conditions are the same as in (A), except that a control involving addition of peptide 2 without Chariot reagent has been added.

(D) Peak anti-CD3-induced Ca^{2+} elevation in Jurkat cells treated with peptides as in (C) (mean ± SEM, seven experiments, mean 81 cells per sample per experiment).

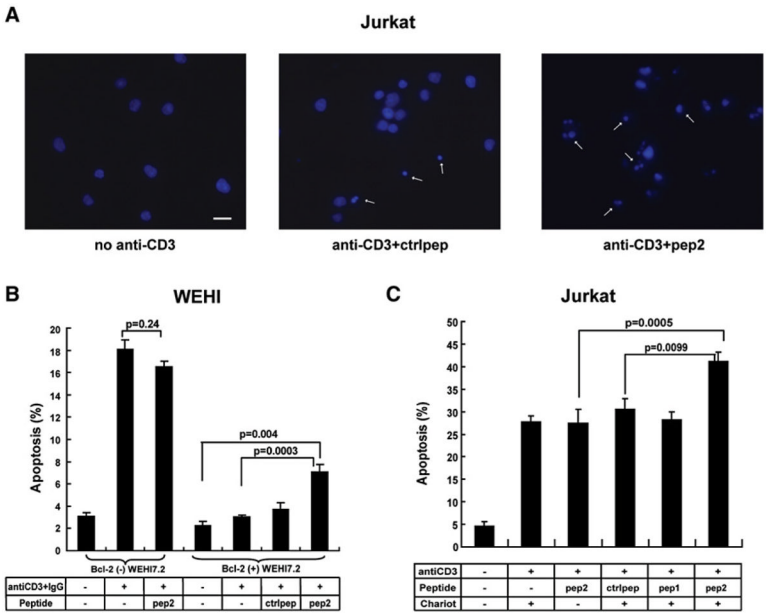

Figure 7. Peptide 2 Enhances Anti-CD3-Induced Apoptosis in Bcl-2-Positive Cells

(A) Typical apoptotic nuclear morphology (arrow, Hoechst 33342 stain) 24 hr after 5 μg/ml anti-CD3 treatment of Jurkat cells. Scale bars, 10 μm.

(B) Bcl-2(−) and Bcl-2(+) WEHI7.2 cells were preincubated ± 60 μM peptides plus Chariot reagent and then incubated with 20 μg/ml anti-CD3 for 24 hr. Symbols represent the percentage of cells (mean ± SEM) with apoptotic nuclei in three experiments for Bcl-2(−) and five experiments for Bcl-2(+) cells (200 cells counted per coverslip).

(C) Jurkat cells were preincubated ± 60 μM peptides ± Chariot reagent and then incubated with 5 μg/ml anti-CD3 for 24 hr. Symbols represent the percentage of cells (mean ± SEM) with apoptotic nuclei in five experiments (240 cells counted per coverslip).